Materials Science in Additive Manufacturing

ORIGINAL RESEARCH ARTICLE

From 3D printed molds to bioprinted scaffolds: A hybrid material extrusion and vat polymerization bioprinting approach for soft matter constructs

Zainab N. Khan[1†], Hamed I. Albalawi[1†], Alexander U. Valle-Pérez[1], Ali Aldoukhi[1], Noofa Hammad[1], Elena Herrera-Ponce de León[1], Sherin Abdelrahman[1], Charlotte A. E. Hauser[1,2*]

[1]Laboratory for Nanomedicine, Division of Biological and Environmental Science and Engineering, King Abdullah University for Science and Technology, Thuwal, 23955- 6900, Saudi Arabia

[2]Computational Bioscience Research Center, King Abdullah University of Science and Technology, Thuwal 23955, Saudi Arabia

Abstract

Three-dimensional (3D) bioprinting methods vary in difficulty and complexity depending on the application desired and biomaterials used. 3D biofabrication is gaining increased traction with enhanced additive manufacturing technologies. Yet, high print resolution and efficiency for the fabrication of complex constructs still prove to be challenging. An intricate balance between biomaterial composition, machine maneuverability, and extrusion mechanism is required. While soft bioinks are highly desirable when used as a biodegradable scaffold material for tissue and organ fabrication, mechanical stiffness and shape fidelity are often compromised. Alternately, post-printing ultraviolet and chemical crosslinking processes improve fidelity but threaten cell viability. Herein, we propose a hybrid fabrication approach to facilitate 3D bioprinting using soft bioinks with instantaneous gelation properties while maintaining shape fidelity for tissue and organ structures of complex geometries. The approach entails a multi-step "3D Printed Molds to Scaffolds" method, which uses additive manufacturing to create accurate negative support structures for the desired construct. A tissue or organ model is first designed in computer-aided design (CAD) modeling software to create a negative mold structure of the desired tissue or organ. Using a Formlabs® SLA 3D printer, the negative mold is fabricated at desired scale using a biocompatible elastic resin. Then, a robotic 3D bioprinting system is loaded with a sliced g-code of the CAD model. The robot start position is aligned with the placement of the fabricated mold on the printbed. Microfluidic pumps deliver three solutions through a customized nozzle to extrude peptide bioink, which gels instantaneously. The initial layers of the structure are formed within the mold to create a solid foundation of the construct. The hybrid approach was found to enhance fidelity considerably and enabled the printing of a complex human ear structure. It is promising for tissue and organ fabrication as it offers a cost-effective support structure without increasing printing time. It could also be used as a rapid prototyping approach for researchers who do not have access to 3D bioprinting systems. Biofabrication, from printed molds to bioprinted

†These authors contributed equally to this work.

***Corresponding author:** Charlotte A. E. Hauser (charlotte.hauser@kaust.edu.sa)

Citation: Khan ZN, Albalawi HI, Valle-Pérez AU, *et al.*, 2022, From 3D printed molds to bioprinted scaffolds: A hybrid material extrusion and vat polymerization bioprinting approach for soft matter constructs. *Mater Sci Add Manuf*, 1(1): 7. https://doi.org/10.18063/msam.v1i1.7

Received: March 4, 2022

Accepted: March 11, 2022

Published Online: March 28, 2022

scaffolds, will potentially enhance the printing experience with soft bioinks while preserving cell durability and viability.

Keywords: 3D Bioprinting; Vat polymerization; Tissue engineering; 3D molds; Peptide hydrogels; Soft bioinks

1. Introduction

Conventional additive manufacturing technologies can be classified into three main technologies: material extrusion, material jetting and vat polymerization[1-7]. In addition, they can be combined to give rise to alternative biofabrication strategies, such as freeform reversible embedding of suspended hydrogels printing[8]. These biofabrication approaches present several advantages as they are compatible with an extensive plethora of scaffolding materials and cells[9]. However, the inherent complexity in the three-dimensional (3D) biofabrication of structures like real-scale organs still poses several challenges which could be overcome by incorporating alternative elements such as molds and supports during the 3D bioprinting process. Hence, the integration of support structures during the biofabrication process of 3D bioprinted structures can be exploited.

A noteworthy example of 3D bioprinting using the aid of molds could be the Method A of CoraPrint developed by Albalawi *et al.*[10]. It is a molding process, which consists of the scanning of a live coral, modification of its 3D geometry, 3D printing of the coral skeleton with commercial polylactic acid filament, and creating a silicone mold for Calcium Carbonate Photoinitiated ink. The time from start to finish for the molding process is approximately 4-5 h, excluding the printing time needed for the positive mold model and the post-molding curing time, which both are dependent on the desired size of the coral structure. The efficiency of this method was confirmed in model coral models of out plant size and thus indicate the possibility of the creation of coral replicas at an efficient rate for large-scale production. Once created, a mold can be used several times and subsequent structures can be molded within 10 min. In regard to different coral species with varying structural geometry and size, this method offers a solution in terms of support and definition. The molding can support the structures of field deployment size while the first step of 3D printing can preserve the sophisticated geometries of the coral. Another advantage mentioned is the lack of use of a large infrastructure setup for transportation since the molds can be smoothly transported to various locations.

Another example of molds used in bioprinting is perfusable conducts[11]. The mold fabricated was composed of Polydimethylsiloxane elastomer and a Pluronic F127/thrombin blend fugitive ink. The cell-laden ink made of gelatin, fibrinogen, transglutaminase, and thrombin, was cast into the mold and the sacrificial ink was perfused out of the construct. The mold was used because, in the former process of indirect extrusion-based bioprinting (EBB), the thick bioprinted constructs could not be perfused directly; therefore, the bioprinted constructs were limited in long-term culture time or increased thickness despite accomplishing the fabrication of multi-layered constructs. However, indirect EBB has already been explored for bioprinting vascular models, which consists of using fugitive or sacrificial inks. These inks are ejected in the form of solid tubular structures, followed by other hydrogels as layers are formed in the adjacent bulk. The sacrificial ink is then removed by dissolution, leaving behind a hollow construct in the gel.

According to Janarthanan *et al.*, printing self-supported multi-layered constructs with biocompatible hydrogels is considered one of the major challenges in extrusion-based 3D bioprinting[12]. Bioinks must have sufficient mechanical stability in soft tissue and organ regeneration post-printing. Furthermore, there are many issues besides post-printing stability that include cell damage, porosity with interconnected microporous structures, and cross-linking density. By overcoming these issues, the capability of cell migration as well as the fine-tuning of their rheological and swelling properties can be achieved. In addition, it is very important to ensure that the bioinks used in 3D bioprinting are highly biocompatible in order to accommodate living cells and to be mechanically stable post-printing. Furthermore, these inks require a high level of resolution during printing[13,14]. On the other hand, the impact of bioink viscosity on 3D printing and the results revealed that viscosity and printing speed are interdependent by applying pressure to obtain a high level of stability of the printed structure[15]. Furthermore, other results indicate that there are enhancements in the mechanical properties of the printed constructs as well as high stability post-printing[16]. However, this study showed a slight decrease in cell viability post-printing when examined with human mesenchymal stem cells (MSC).

Regarding bioinks, aromatic and non-aromatic tetra-peptide amphiphiles, Ac-Ile-Ile-Phe-Lys-NH_2 (IIFK), Ac-Ile-Ile-Cha-Lys-NH_2 (IIZK), and Ac-Ile-Cha-Cha-Lys-

NH_2 (IZZK) peptide bioinks for bioprinting applications have been reported[17]. These peptides have been rationally designed as ultrashort and self-assembling are considered to be an encouraging class of biomaterials as they address several limitations that are affiliated with bioinks[18]. Amphiphilic peptides are composed of 3 – 7 amino acids in length and they self-assemble under physiological conditions to form hydrogels from nanofibers that meticulously resemble fibers within the extracellular matrix. The characteristics previously mentioned make ultrashort peptides a suitable biomaterial for regenerative medicine applications and tissue engineering[19]. Susapto *et al.* have demonstrated the excellent tunable mechanical properties of their bioinks, thus making them suitable as robust bioinks for 3D bioprinting[17]. These bioinks avoid cell compromising abrasive conditions like chemical treatments or ultraviolet (UV) cross-linking during the printing process. Their peptide bioinks verified an instantly solidifying cell-embedding 3D bioprinting process under physiological conditions at a low, cost-effective bioink concentration. These peptide bioinks are capable of being considered superior due to their biocompatible, body-like, synthetic nature, and support of an automated cell printing process.

The main classification of hydrogels is based on their sources - natural, synthetic, and hybrid. Natural hydrogels can be obtained from proteins (elastin, collagen, fibrin, silk fibroin, and gelatin), polysaccharides, and decellularized tissues[20]. Synthetic hydrogels display more versatile and easily controlled physical and chemical properties when compared to natural-origin hydrogels[21]. Hybrid hydrogels, on the other hand, are a mixture of natural and synthetic hydrogels, which incorporate structures with desirable characteristics[22]. Hydrogels can also be classified by their structural integrity (durable and biodegradable). Durable hydrogels are mostly synthetic and mechanically stronger in comparison to hydrogels of natural origin, while biodegradable hydrogels are natural polymers, commonly non-toxic, and demonstrate minimal adverse effects compared to synthetic alternatives[23]. For the hydrogels to function properly, they are expected to meet several design criteria so that they can stimulate new tissue formation and induce minimal to no immune reaction from the recipient. The selection of these hydrogels depends primarily on their physical parameters (mechanical properties, biodegradability or bioresorbability, porosity, and swelling) and biological performance (biocompatibility, cell adhesion, vascularization, and bioactivity)[20].

On the other hand, a fast hydrogel projection stereolithography (SLA) technology (FLOAT), which allows the fabrication of centimeter-sized and multi-scale solid hydrogel models in minutes has been reported[24]. This was achieved by precisely controlling the photopolymerization condition and establishing low suction force-driven, high-velocity flow of the hydrogel prepolymer that backs up the continuous replenishment of the prepolymer solution below the curing part and the nonstop part growth. The process is unique for the hydrogel prepolymer without externally supplemented oxygen. The rapid printing of centimeter-sized hydrogel models using FLOAT has exhibited a significant reduction in deformation and cellular injury caused by prolonged exposure to environmental stresses in layer-by-layer-based printing methods.

Meanwhile, the additional degrees of freedom of robots have increased the capability, quality, and productivity of traditional 3D fabrication[25]. One of the major issues in conventional additive manufacturing addressed by Bhatt *et al.* is that printing structural layers perpendicularly limits the types of geometry that can be printed[26]. Robot-assisted additive manufacturing allows for change of directions during 3D fabrication, thus making fabrication of complex geometry feasible[27]. A study by Song *et al.* concluded that printing in tilted orientations can help avoid the staircase effect that occurs due to the approximation of planar layers for highly curved geometry[28]. Moreover, a 3D printing robot can decrease or eliminate, in some cases, the need for support structures due to its ability to orient the printing tool to reach the objects from different angles. In other words, the tool path of the deposition head can be non-planar in space[26]. This survey paper, Bhatt *et al.*, also mentioned two other advantages of utilizing robots as 3D printers in manufacturing which are scalability and mobility of the printed structures[26]. For instance, a recent study highlights the application of additive manufacturing in the fabrication of lateral flow assays for the rapid in-field detection of COVID-19[29].

In this study, we combined the advancing technologies of additive manufacturing, 3D biofabrication, and robotics to develop a hybrid fabrication approach for high-quality printing of cellular bio-scaffolds with soft bioinks (Figure 1). We offer a multi-step method involving SLA and extrusion-based printing technologies to precisely engineer customizable mold support structures to improve printing resolution and mechanical fidelity. Our process is implemented by 3D bioprinting a human ear model with peptide-based bioink embedded with MSCs and assessing the 3D scaffold for mechanical fidelity and cell viability.

2. Method

We proposed a hybrid fabrication approach to enable 3D bioprinting using soft bioink materials, such as peptide hydrogels, for the printing of complex organ and tissue structures. The hybrid approach involves a multi-step "3D

Printed Molds to Scaffolds" process: reverse engineering, 3D bioprinter setup, and scaffold fabrication (Figure 2A-E).

2.1. Reverse engineering to create a 3D printed mold

First, a desired tissue or organ model is designed in a suitable computer-aided design (CAD) modeling software or scanned with a 3D scanner. The CAD model is modified for discrepancies and then used to create a negative model for the desired construct using the CAD modeling software. A block is designed around the selected 3D model and then extruded bi-directionally from its cross-sectional center. Considering the final material property, the scale and depth of the desired shape should be in the range of 3 – 4 mm, which is a suitable thickness to maintain the flexibility of the mold. A mold of complex shapes should have at least 2 mm in thickness from all sides to avoid any tear and maintain reusability.

The desired structure is then subtracted from the block to form a negative imprint on the surface. This results in a reverse-engineered support structure, preserving the accurate geometries of the desired construct to be printed. Next, the support structure model is modified to create additional support thickness, encompassing all features of the structure. Further design modifications are made based on the shape's geometric details to ensure a seamless printing process.

For design assessment, an assembly is created by merging the negative mold with the positive desired shape to ensure perfect alignment for the added support features. The negative mold is then 3D printed using a SLA 3D printer with a flexible biocompatible material. Fabricating the mold through 3D printing preserves the intricate features of the model, which will later be essential in the 3D bioprinting process to create a cell-laden scaffold.

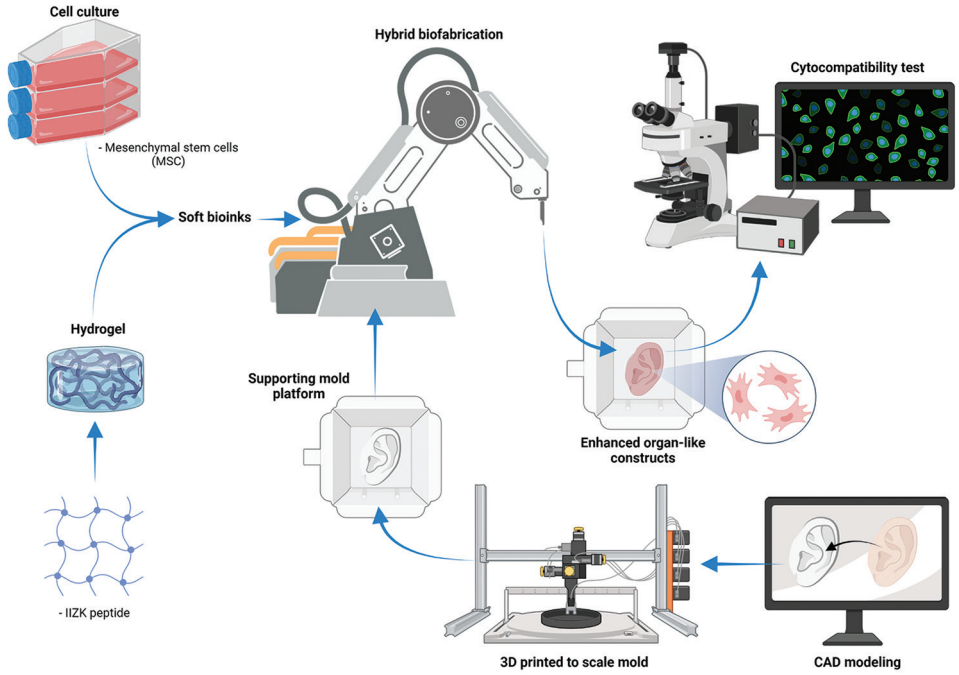

Figure 1. General overview of the process flow.

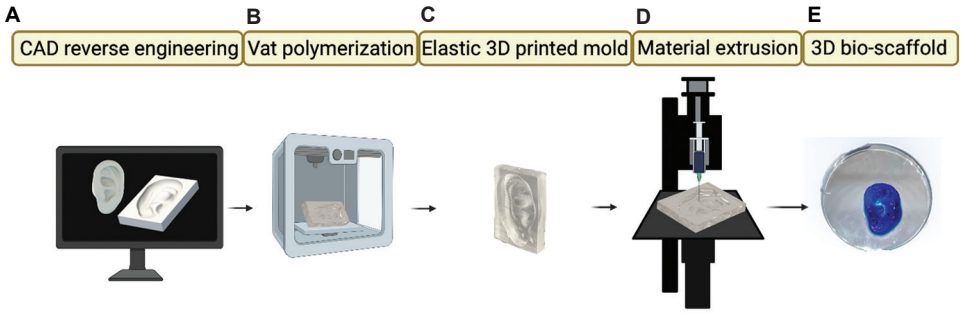

Figure 2. (A-E) A schematic figure showing the multi-step engineering process from "3D Printed Molds to Scaffolds".

To demonstrate this approach, an open-source CAD model of a human ear was obtained and modified to create a negative mold using NX SIEMENS software, as described in the process above. A scale of 1:1 ratio was maintained to keep the model as realistic as possible. After implementing a cut into the extruded block and adding feature modifications, the mold was 3D printed with a Formlabs® 3B+ 3D printer using biocompatible elastic resin.

Finite element analysis (FEA) was performed to test the design's flexibility further and ease of releasing the desired structure after 3D printing. Using the NX SIEMENS software, the material was set to the selected material elasticity of the 3D printed mold. The mold was 3D meshed and constrained from the bottom side and was set to experience a force against the upper side with F=15 N (Figure 3B).

2.2. Parameter optimization for 3D bioprinter and G-code

For seamless material extrusion into the mold, the g-code file was optimized to conform to the mold profile. First, the CAD model for the human ear model was sliced using Cura slicer software and adjusted in terms of print speed, layer height, and orientation to be suitable for 3D bioprinting. Then, the g-code was modified to ensure free movement by removing any features that would cause collision and adding layers where necessary to maintain the desired shape. Bottom layers of the g-code were removed to allow the mold to serve its purpose. Noteworthy, for non-symmetrical shapes like the human ear, the positive CAD model has to be mirrored along the horizontal X-axis to ensure that the inner features align with those of the negative mold. For orientation, it is essential that the g-code path aligns with the position of the mold placed on the printbed. This was done by creating a user-defined home position for the robotic arm. The mold was then fixed to the printbed such that its start point in the g-code aligned with the user-defined home position. Likewise, in the Repetier printing software, the printbed dimensions were entered accurately, and the g-code file was loaded to be at the center of the user-defined home position.

Our in-house developed robotic 3D bioprinting system[30,31] also required optimization to print with the mold. The robotic 3D bioprinter was prepared for printing with peptide-based hydrogels to assess suitability of the molds for soft bioink materials. For optimal material extrusion into the mold, the microfluidic pumps were programmed with alternating square wave flow profiles to enable automated time-dependent pumping of the solutions. The optimization process for this parameter was developed in a previously reported study[32]. The square wave profile for the peptide hydrogel solution was set to a range of 55 – 60 µl/min with a 75% duty cycle and a period of 80 s. For the phosphate-buffered soline (PBS), the square wave profile had a range of 15 – 20 µl/min with a 25% duty cycle and a period of 80 s. The microfluidic ink delivery system was loaded with peptide hydrogel and PBS to facilitate bioink formation.

2.3. Creating the 3D bioprinted scaffolds

To evaluate shape fidelity and biocompatibility of 3D bioprinted structures with mold support, a human ear model was 3D bioprinted with peptide bioink. The robotic 3D bioprinter was mounted with a homemade dual coaxial nozzle consisting of three inlets as described previously[17]. One inlet is for the peptide solution, another one for the PBS buffer and a third inlet for the cells. Initially, the molds were tested for shape fidelity by printing an acellular 3D human ear construct. In this experiment, IVZK peptide was dissolved in water at an initial concentration of 13 mg/ml. Furthermore, a 5× PBS buffer was used to induce gelation and solidify the hydrogel before extrusion. All solutions were loaded into the microfluidics pumps and extruded through the nozzle using the automated pumping program described earlier. The constructs were left to solidify inside the mold for 30 min after printing. They were then removed from the mold and shape fidelity was subjectively assessed in comparison to the 3D model design.

2.4. Cell bioprinting and bioimaging

Experiments were done to assess the suitability of using the mold support method with cellular constructs. Initially, IIZK peptide was dissolved in sterile water at an initial concentration of 13 mg/ml and loaded into the microfluidics pumps along with a sterile 5×PBS buffer. The mold was washed with 70% ethanol and sterilized for 30 min under UV light before bioprinting. MSCs were cultured in T175 flasks until they reached 95% confluency at passage eight. The cells were suspended in a 1×PBS buffer supplemented with 5% FBS. Cells were loaded into the microfluidics pumps and extruded at a constant flow rate of 15 µl/min. After printing, the constructs were left in the mold and incubated overnight at 37°C with Dulbecco's Modified Eagle Medium supplemented with 5% L-glutamine. The constructs were removed from the mold the next day. At day 1, cell viability was assessed using live-dead imaging staining with confocal microscopy.

3. Results

Fabrication of the optimal mold for 3D bioprinting was found to be an experimental process that required several iterations to achieve quality results. The first iteration was fabricated with standard resin, which is a stiff and rigid

material. This proved to pose a problem when removing a print from the mold post-printing. It also disrupted material flow in the bottom layers as the structure details would be more defined. To combat this, Formlabs® elastic 50A resin was used. This facilitated the removal process considerably. It is also worth mentioning that this resin is biocompatible, which further supports cellular bioprinting. However, with the flexible mold, it was observed that the bottom printed layer had a tendency to attach to the base of the mold, which was undesirable, as it would negatively affect print quality. This was resolved by reducing the mold thickness to create a pop-in, pop-out effect. This further improved the removal process and allowed the structure to maintain its shape.

The FEA study showed the displacement and the Von-Mises result (Figure 3A and B). The Von-Mises was found to be equal to 2.11 MPa, which is lower than the yield strength of the material, equivalent to 3.23 MPa (Figure 3C). The study results were promising as the displacement was equivalent to 25.97 mm, indicating that a regular force of 1.5 kg can result in 25.97 mm flexure in the mold (Figure 3D). This study suggested that the structure's material withstands the peeling force that is to be experienced after 3D printing with no damage to the structure or the inner desired features.

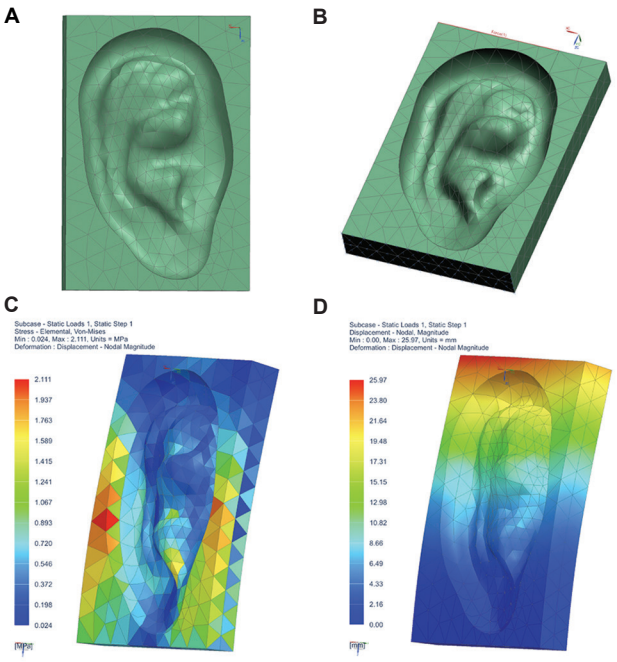

Figure 3. A finite element analysis (FEA) study on the human ear mold model. (A) A CAD model of a human ear model with applied tetrahedral mesh. (B) The constraint from the bottom side of the mold and an applied force against the upper side with F=15 N. (C) The Von-Mises result equal to 2.11 MPa, which is lower than the yield strength of the selected material, equivalent to 3.23 MPa. (D) The displacement result, which indicates that a regular force of 1.5 kg can result in 25.97 mm flexure in the mold.

Acellular human ear constructs were 3D bioprinted with peptide-based bioink to form a soft bioink scaffold (Figure 4A). Automated time-dependent extrusion of the bioink enabled consistent flow throughout printing, which was essential for the construct to take a well-formed shape. G-code optimization also facilitated a collision-free printing experience. Post-printing, the constructs were evaluated for shape fidelity and cell viability. In terms of mechanical structure, the 3D bioprinted full human ear scaffold was found to maintain its shape and easily reconstruct the complex geometry of the model despite its small-scale size.

The 3D bioprinting of cellular scaffolds was done in the mold support structures and is demonstrated in Figure 4A, after overnight incubation and removal from the mold. The 3D scaffold maintained shape fidelity after overnight incubation in culture media. Moreover, live-dead imaging at day 1 of culture showed high cell viability. This further confirms the biocompatibility of the mold resin material and verifies the practicality of use for cellular 3D bioprinting. Confocal images of the cellular scaffold were taken (Figure 4B and C). In addition, the z-stacking video of the live-dead imaging is provided as Supplementary File.

4. Discussion

Our proposed hybrid method, "From 3D Printed Molds to Scaffolds," was found to be an effective, cost-efficient technique to fabricate complex 3D cellular structures with soft bioinks. Other methods include the application of a thermo reversible biocompatible support to enhance

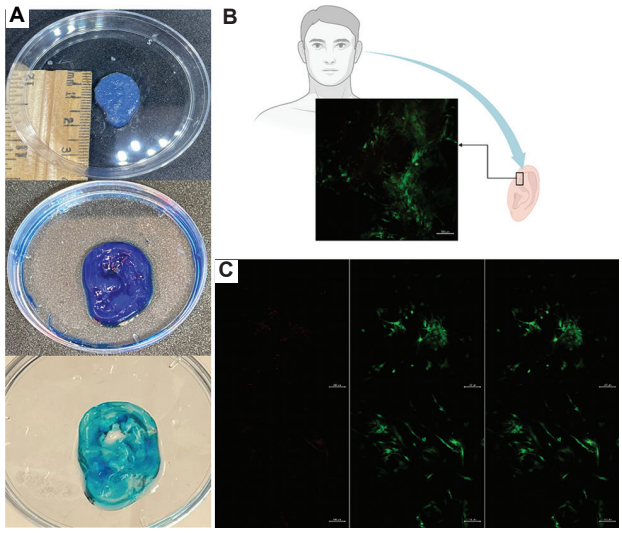

Figure 4. Bioprinted human ear with the hybrid biofabrication technique. (A) The acellular construct was printed over the designed mold. (B) The Live/Dead cytocompatibility assay was carried out to assess cell viability after 1 day. (C) Split-view representation of the dead cells (red) and live cells (green) at two different positions from the bioprinted ear.

additive manufacturing by embedding the printed hydrogel within a secondary thermo reversible hydrogel[33,34]. On the other hand, another strategy exploits the addition of self-supporting nanoclay materials like laponite as an internal scaffold biomaterial for fabricating complex structures[34]. In our approach, shape fidelity was considerably improved for peptide-based bioinks as compared to previous studies regarding 3D bioprinting without support structures. In experiments without support, it was only possible to print the human ear model with basic outlined features, yet geometries were not preserved in the construct. Hence, the method proved instrumental in maintaining essential geometries and print resolution. Moreover, our bioprinting approach is not temperature dependent, while the bioprinted construct can be stored within the mold inside of an incubator and then removed, suggesting an alternative strategy for the fabrication of complex 3D bioprinted structures.

Fabrication of the mold went through several iterations to achieve optimal results and appreciate the effectiveness of the presented method. It was concluded that precise modification is essential before mold fabrication to ensure accuracy and reusability of the support structure. FEA analyses with the flexible material were crucial in creating an easy release technique for removing the construct after printing. A further advantage could be taken of the mold's flexibility by reducing its border thickness. A decrease in thickness of 0.3 mm was found to make a considerable difference in the ease of removing the human ear construct. It was also found that a 3-4 mm range is optimal for the thickness and flexibility to be maintained (Figure 3A and B).

Using a commercially available SLA 3D printer with a laser power of 250 mW facilitated the printing of small and highly accurate support structures. In addition, the elastic resin material allowed the fabrication of a precise, highly flexible mold. Resolution and flexibility play an important role in making the method successful. Due to the non-cytotoxicity of the material, the mold can be inserted in the incubator with cells to continue growing. Post-printing, the cells can grow to the fine details of the mold. Further modifications to the design can allow media and nutrition to reach the cells to enhance the post-printing growth.

The automated pumping process for bioink extrusion allowed the construct to take shape during the print without any clogging or disruption. It is worth mentioning that printing tests done without automated pumping produced constructs with looser infills, which made them more fragile and difficult to remove from the mold without causing damage. G-code optimization requires a number of iterations to achieve free movement of the nozzle in the mold without collision. It is essential to slice the g-code with optimal parameters to allow the nozzle movement to conform to the mold profile. In contrast to conventional mold casting, material extrusion into the mold is required in this process to allow homogeneous layering of cells in the construct without negatively impacting viability. It also opens the door for the printing of multi-cellular scaffolds.

Based on the observations from this study, our method is recommended as a supplementary approach for 3D bioprinting with soft bioinks to enhance mechanical stability in fabrication without compromising cell viability. A valuable advantage of this approach is time efficiency and material conservation, as it removes the need for incorporating supports during printing. As the molds can be created in advance and easily be reused after cleaning with ethanol, the printing process is not additionally lengthened, and cell viability is not jeopardized. Alternative use of this method could be in the absence of a 3D bioprinter, where 3D molds can be used to hold cell-laden soft bioink scaffolds and allow them to take shape over time. Due to the agile fabrication process, edits and customization can be easily made and done repeatedly.

Our data also suggests that the Formlabs® elastic resin shows low cytotoxic effects when incubated with cells overnight, since the number of live cells was considerably higher than dead cells (Figure 4B). This opens the possibility for printing with softer materials that require a longer time to solidify and harden to maintain high shape fidelity. Molds could also be created from biodegradable materials to disintegrate over time as cellular scaffolds take their own shape. From this aspect, four-dimensional bioprinting and long-term shape fabrication can be further explored.

5. Conclusion

The proposed "3D Printed Molds to Scaffolds" method is a practical additive manufacturing approach to improve biofabrication of soft material constructs. In the future, traditional EBB methods will need to be paired with such techniques to make tissue and organ fabrication a wide-scale reality. The hybrid approach enables the growth of cells, which highlights its potential role in biofabrication. 3D bioprinted human ear scaffolds were observed to maintain shape fidelity and cell viability. Automated time-dependent pumping of bioink and optimized g-code parameters were essential in achieving successful prints with the mold. Moreover, the proposed method was optimized and improved to achieve the intended goal.

Funding

The research reported in this publication was supported by funding from King Abdullah University of Science and Technology (KAUST).

Conflict of interest

There are no conflicts to declare.

Author contributions

Conceptualization: Hamed I. Albalawi, Zainab N. Khan, Sherin Abdelrahman, Charlotte A. E. Hauser

Investigation: Zainab N. Khan, Hamed I. Albalawi, Alexander U. Valle-Pérez, Ali Aldoukhi, Noofa Hammad, Elena Herrera-Ponce de León

Methodology: Hamed I. Albalawi, Zainab N. Khan

Software: Zainab N. Khan, Noofa Hammad

Supervision: Charlotte A. E. Hauser

Validation: Ali Aldoukhi, Alexander U. Valle-Pérez, Zainab N. Khan

Visualization: Alexander U. Valle-Pérez, Hamed I. Albalawi

Writing – original draft: Zainab N. Khan, Hamed I. Albalawi, Alexander U. Valle-Pérez, Ali Aldoukhi, Noofa Hammad, Elena Herrera-Ponce de León

Writing – review & editing: Zainab N. Khan, Charlotte A. E. Hauser

References

1. Murphy SV, Atala A, 2014, 3D bioprinting of tissues and organs. *Nat Biotechnol*, 32: 773–785.

   https://doi.org/10.1038/nbt.2958

2. Jiang T, Munguia-Lopez JG, Flores-Torres S, *et al.* 2019, Extrusion bioprinting of soft materials: An emerging technique for biological model fabrication. *Appl Phys Rev*, 6: 011310.

   https://doi.org/10.1063/1.5059393

3. Li X, Liu B, Pei B, *et al.*, 2020, Inkjet bioprinting of biomaterials. *Chem Rev*, 120: 10793-10833.

   https://doi.org/10.1021/acs.chemrev.0c00008

4. Ng WL, Lee JM, Yeong WY, *et al.*, 2017, Microvalve-based bioprinting-process, bio-inks and applications. *Biomater Sci*, 5: 632–647.

5. Dou C, Perez V, Qu J, *et al.*, 2021, A state-of-the-art review of laser-assisted bioprinting and its future research trends. *Chem Bio Eng Rev*, 8: 517–534.

   https://doi.org/10.1002/cben.202000037

6. Ng WL, Lee JM, Zhou M, *et al.*, 2020, Vat polymerization-based bioprinting process, materials, applications and regulatory challenges. *Biofabrication*, 12: 022001.

   https://doi.org/10.1088/1758-5090/ab6034

7. Li W, Mille LS, Robledo JA, *et al.*, 2020, Recent advances in formulating and processing biomaterial inks for vat polymerization-based 3D printing. *Adv Healthc Mater*, 9: 2000156.

   https://doi.org/10.1002/adhm.202000156

8. Ahangar P, Cooke ME, Weber MH, *et al.*, 2019. Current biomedical applications of 3D printing and additive manufacturing. *Appl Sci*, 9: 1713.

9. Guzzi EA, Tibbitt MW, 2020, Additive manufacturing of precision biomaterials. *Adv Mater*, 32: 1901994.

10. Albalawi HI, Khan ZN, Valle-Pérez AU, *et al.*, 2021, Sustainable and eco-friendly coral restoration through 3d printing and fabrication. *ACS Sustain Chem Eng*, 9: 12634-12645.

11. Sasmal P, Datta P, Wu Y, *et al.*, 2018, 3D bioprinting for modelling vasculature. *Microphysiol Syst*, 2: 9.

    https://doi.org/10.21037/mps.2018.10.02

12. Janarthanan G, Shin HS, Kim IG, *et al.*, 2020, Self-crosslinking hyaluronic acid–carboxymethylcellulose hydrogel enhances multilayered 3D-printed construct shape integrity and mechanical stability for soft tissue engineering. *Biofabrication*, 12: 045026.

    https://doi.org/10.1088/1758-5090/aba2f7

13. Gopinathan J, Noh I, 2018, Recent trends in bioinks for 3D printing. *Biomater Res*, 22: 11.

14. Avila-Ramírez A, Valle-Pérez AU, Susapto HH, *et al.*, 2021, Ecologically friendly biofunctional ink for reconstruction of rigid living systems under wet conditions. *In J Bioprint*, 7: 398.

    https://doi.org/10.18063/ijb.v7i4.398

15. Tirella A, Orsini A, Vozzi G, *et al.*, 2009, A phase diagram for microfabrication of geometrically controlled hydrogel scaffolds. *Biofabrication*, 1: 045002.

    https://doi.org/10.1088/1758-5082/1/4/045002

16. Poldervaart MT, Goversen B, de Ruijter M, *et al.*, 2017, 3D bioprinting of methacrylated hyaluronic acid (MeHA) hydrogel with intrinsic osteogenicity. *PLoS One*, 12: e0177628.

    https://doi.org/10.1371/journal.pone.0177628

17. Susapto HH, Alhattab D, Abdelrahman S, *et al.*, 2021, Ultrashort peptide bioinks support automated printing of large-scale constructs assuring long-term survival of printed tissue constructs. *Nano Lett*, 21: 2719–2729.

    https://doi.org/10.1021/acs.nanolett.0c04426

18. Hauser CA, Deng R, Mishra A, *et al.*, 2011, Natural tri- to hexapeptides self-assemble in water to amyloid β-type fiber aggregates by unexpected á-helical intermediate structures. *Proc Natl Acad Sci*, 108: 1361–1366.

    https://doi.org/10.1073/pnas.1014796108

19. Loo Y, Lakshmanan A, Ni M, *et al.*, 2015, Peptide bioink: Self-assembling nanofibrous scaffolds for three-dimensional

organotypic cultures. *Nano Lett*, 15: 6919–6925.

https://doi.org/10.1021/acs.nanolett.5b02859

20. Advincula RC, Dizon JR, Caldona EB, *et al*., 2021, On the progress of 3D-printed hydrogels for tissue engineering. *MRS Commun*, 11: 539–553.

https://doi.org/10.1557/s43579-021-00069-1

21. Spicer CD, 2020, Hydrogel scaffolds for tissue engineering: The importance of polymer choice. *Polym Chem*, 11: 184–219.

22. Naahidi S, Jafari M, Logan M, *et al*., 2017, Biocompatibility of hydrogel-based scaffolds for tissue engineering applications. *Biotechnol Adv*, 35: 530-544.

https://doi.org/10.1016/j.biotechadv.2017.05.006

23. Khansari MM, Sorokina LV, Mukherjee P, *et al*., 2017, Classification of hydrogels based on their source: A review and application in stem cell regulation. *JOM*, 69: 1340–1347.

https://doi.org/10.1007/s11837-017-2412-9

24. Anandakrishnan N, Ye H, Guo Z, *et al*., 2020, Fast 3D printing of large-scale biocompatible hydrogel models. *BioRxiv*, 2020: 345660.

https://doi.org/10.1101/2020.10.22.345660

25. Morioka M, Sakakibara S, 2010, A new cell production assembly system with human-robot cooperation. *CIRP Ann*, 59: 9–12.

26. Bhatt PM, Malhan RK, Shembekar AV, *et al*., 2020, Expanding capabilities of additive manufacturing through use of robotics technologies: A survey. *Addit Manuf*, 31: 100933.

https://doi.org/10.1016/j.addma.2019.100933

27. Urhal P, Weightman A, Diver C, *et al*., 2019, Robot assisted additive manufacturing: A review. *Robot. Comput Integr Manuf*, 59: 335-345.

https://doi.org/10.1016/j.rcim.2019.05.005

28. Song X, Pan Y, Chen Y, 2015, Development of a low-cost parallel kinematic machine for multidirectional additive manufacturing. *J Manuf Sci Eng*, 137: 021005.

https://doi.org/10.1115/1.4028897

29. Alrashoudi AA, Albalawi HI, Aldoukhi AH, *et al*., 2021, Fabrication of a lateral flow assay for rapid in-field detection of COVID-19 antibodies using additive manufacturing printing technologies. *Int J Bioprint*, 7: 399.

https://doi.org/10.18063/ijb.v7i4.399

30. Khan Z, Kahin K, Rauf S, *et al*., 2018, Optimization of a 3D bioprinting process using ultrashort peptide bioinks. *Int J Bioprint*, 5: 173.

https://doi.org/10.18063/ijb.v5i1.173

31. Kahin K, Khan Z, Albagami M, *et al*., 2019, Development of a robotic 3D bioprinting and microfluidic pumping system for tissue and organ engineering. In: Gray BL, Becker H, editors. Microfluidics, BioMEMS, and Medical Microsystems XVII (SPIE, 2019).

https://doi.org/10.1117/12.2507237

32. Khan Z, Kahin K, Hauser C, 2021, Time-dependent pulsing of microfluidic pumps to enhance 3D bioprinting of peptide bioinks. In: Gray BL, Becker H, editors. Microfluidics, BioMEMS, and Medical Microsystems XIX (SPIE, 2021).

https://doi.org/10.1117/12.2578830

33. Ng WL, Chua CK, Shen YF, 2019, Print me an organ! Why we are not there yet. *Prog Polym Sci*, 97: 101145.

https://doi.org/10.1016/j.progpolymsci.2019.101145

34. Hinton TJ, Jallerat Q, Palchesko RN, *et al*., 2015, Three-dimensional printing of complex biological structures by freeform reversible embedding of suspended hydrogels. *Sci Adv*, 1: e1500758.

https://doi.org/10.1126/sciadv.1500758